Atomic-scale measurement of ultraslow Li motions in glassy LiAlSi$_2$O$_6$ by two-time ^{6}Li spin-alignment echo NMR correlation spectroscopy

M. Wilkening,[*] A. Kuhn, and P. Heitjans[†]

Institute of Physical Chemistry and Electrochemistry, and Center for Solid State Chemistry and New Materials,
Leibniz University Hannover, Callinstraße 3a, D-30167 Hannover, Germany
(Received 21 May 2008; published 12 August 2008)

^{6}Li spin-alignment echo (SAE) nuclear-magnetic-resonance (NMR) spectroscopy is used to monitor single-particle two-time correlation functions in LiAlSi$_2$O$_6$ glass. The method, here applied in the temperature range from 300 to 400 K, is sensitive to ultraslow Li hopping processes with rates ($1/\tau_{SAE}$) down to 10 jumps/s. The use of a sample with natural ^{6}Li abundance allowed the measurement of pure NMR spin-alignment echoes which are damped with increasing mixing time exclusively by slow Li jumps, i.e., free of influences arising from, e.g., interfering spin-diffusion effects. The considerably stretched correlation functions reveal the presence of a broad distribution of jump rates. The results are comprehensively compared with those recently obtained from both ^{7}Li SAE and ^{7}Li spin-lattice relaxation NMR as well as from dc conductivity measurements. Interestingly, the activation energy of the latter, which are sensitive to long-range Li transport parameters, is in good agreement with that microscopically probed by ^{6}Li SAE NMR, here.

I. INTRODUCTION

In the course of developing powerful secondary Li batteries[1–8] being promising for future energy storage, disordered ion conductors, i.e., highly defective crystalline (e.g., nanocrystalline) or amorphous materials, will increasingly be considered as solid electrolytes or electrodes. This is due to the often found observation that structurally disordered Li conductors exhibit exceptionally fast ionic diffusivity as compared to their low-defective crystalline counterparts.[9–14] Understanding the basics of transport phenomena in such materials in more detail is indispensable in effective battery research. In this context, it will be useful to study Li diffusion over a preferably large dynamic range, i.e., including also extremely slow cation motions. Lithium solid-state nuclear magnetic resonance (NMR) offers a large pool of different techniques being sensitive to both micro- and macroscopic transport properties. Advantageous over already well-established Li NMR methods[15–19] is the use of ^{7}Li stimulated echo, or more precisely, spin-alignment echo (SAE) NMR which has so far been applied mainly to crystalline Li conductors.[17,20–32] Similar to modern two-dimensional ^{6}Li and ^{7}Li exchange NMR spectroscopy,[33–38] ^{7}Li SAE NMR is sensitive to extremely slow cation exchange processes and gives access to diffusion parameters from a microscopic point of view. Thus, it is possible to record single-particle motional correlation functions,[39] from which the atomic jump rate can be directly obtained, i.e., without the help of a diffusion model.[21–27]

In some cases the use of ^{6}Li (spin quantum number $I=1$) is advantageous over ^{7}Li ($I=3/2$) SAE NMR. In particular, this is true when (i) strong ^{7}Li homonuclear dipole-dipole interactions[30] largely influence the generation of pure spin-alignment order necessary to record a single-particle two-time correlation function or (ii) if three- or four-time phase correlation functions have to be measured (see, e.g., Refs. 40–42 for similar NMR measurements on ^{109}Ag). The latter would provide, e.g., information about possible dynamical heterogeneities. Problem (i) can be overcome in ^{7}Li NMR by using ^{6}Li enriched samples in order to separate the ^{7}Li spins spatially. The natural abundance of the latter is about 92.5%. Problem (ii), however, is still not solved for ^{7}Li as it requires a phase cycling which is experimentally very difficult to realize for a spin-3/2 nucleus.[39] Fortunately, in the case of ^{6}Li, multitime SAE NMR experiments are possible which are in principle identical to those realized earlier for the ^{2}H nucleus which has also a spin quantum number of $I=1$.[43–45] It is worth mentioning that ^{2}H SAE NMR has developed into one of the most powerful NMR methods to study rotational as well as translational deuteron dynamics. In general, the SAE NMR technique takes advantage of the quadrupole interaction between the electrical quadrupole moment Q of the nucleus under investigation and a nonvanishing electric-field gradient (EFG) produced by the charge distribution in the neighborhood of the ion. The technique is sensitive to extremely slow-diffusion processes with jump rates usually ranging from about 1 to 10^4 s^{-1}. While the lower limit is given by the respective NMR spin-lattice relaxation rate, the upper one is determined by the corresponding spin-spin relaxation rate. In the case of a moderate Li conductor this allows the determination of Li jump rates at temperatures which are easily accessible, i.e., in the present ^{6}Li NMR study between 300 and 400 K. When a fast ion conductor is studied the temperature has to be decreased in order to slow down the Li diffusivity. Whereas ^{7}Li and ^{2}H have comparable electrical quadrupole moments, that of ^{6}Li is by a factor of 50 smaller.[46] This has to be taken into account when setting up the NMR experiment (see below).

The present paper emphasizes both the use of two-time ^{6}Li SAE NMR to measure Li jump rates and the application of this technique to a glassy ion conductor. Following our quite recently published NMR study on single crystalline Li$_3$N, see Ref. 26, this is one of the first papers dealing with ^{6}Li SAE NMR. Here, we have chosen LiAlSi$_2$O$_6$ glass as a model substance in which Li diffusivity seems to be rather complex and which was recently investigated by ^{7}Li SAE

NMR (Ref. [31]) so that straightforward comparisons between the two techniques can be made. To our knowledge only a few more ^{7}Li SAE NMR experiments have been applied so far on glassy materials. The first and so far the only ^{6}Li SAE NMR study on a glass *viz* LiPO$_3$ was just published by Faske *et al.*[47] In contrast to that work, in the present study we have used an isotopically nonenriched sample with the natural ^{6}Li abundance of about 7.5%. Thus, spin-diffusion effects caused by dipole-dipole interactions are almost eliminated. The intentionally utilized low natural abundance and the smaller dipolar magnetic and electrical quadrupolar moments of ^{6}Li as compared to the ^{7}Li nucleus usually lead to long measurement periods. However, in the case of glassy LiAlSi$_2$O$_6$ we benefit from the situation that a large amount of material was available and that the corresponding ^{6}Li NMR spin-lattice relaxation times are relatively short as compared to those of other materials (see below).

II. EXPERIMENT

Glassy LiAlSi$_2$O$_6$ was provided by Schott Glaswerke (Germany). It was prepared by mixing appropriate amounts of highly pure Li$_2$CO$_3$, Al$_2$O$_3$, and SiO$_2$.[48,49] Subsequently, the powder was melted and then rapidly roller quenched to obtain the LiAlSi$_2$O$_6$ glass. The final product is fully x-ray amorphous. Devitrification is achieved when the sample is heated at about 1000 K for a few days.[50] After this procedure the well-known x-ray diffraction pattern of crystalline LiAlSi$_2$O$_6$ with the β-spodumene structure has emerged.

A standard MSL 400 NMR spectrometer (Bruker, Germany) was used for the ^{6}Li NMR measurements. ^{6}Li solid echo spectra were recorded via the pulse sequence[51] $\pi/2 - t_e - \pi/2 - t$. The interpulse delay was about 20 μs. Corresponding NMR spectra were obtained after appropriate zero filling by Fourier transformation of the echoes starting from the echo top. ^{6}Li spin-alignment echoes, i.e., sin-sin correlation functions[44] were recorded utilizing the Jeener-Broekaert three-pulse sequence,[52] $\pi/2 - t_p - \pi/4 - t_m - \pi/4 - t$. Appropriate phase cycling, which is known from analogous ^{2}H measurements,[43] was employed to suppress unwanted coherences. The $\pi/2$ pulse length was about 8 μs. The spectrometer was connected to a shimmed Oxford cryomagnet of a nominal field of 9.4 T corresponding to a ^{6}Li resonance frequency of 58 MHz. We have used a commercial broadband probe (Bruker). The temperature of the sample was monitored via an Oxford ITC within an accuracy of about 3 K. Between 32 and 512 scans were accumulated for one ^{6}Li spin-alignment echo. The recycle delay between each echo measurement was at least $5T_1$ where T_1 is the temperature dependent ^{6}Li NMR spin-lattice relaxation time, which was acquired by means of the well-known saturation recovery pulse sequence. T_1 varied between 50 s at room temperature and about 400 ms at 390 K. Therefore, the time needed to record a ^{6}Li two-time correlation function at fixed t_p but for 25 different mixing times t_m ranged between 2.3 days and a few hours.

Conductivity data were recorded by using an HP 4192 impedance analyzer working between 5 Hz and 13 MHz. For this purpose thin specimens (0.5 mm thickness) of the
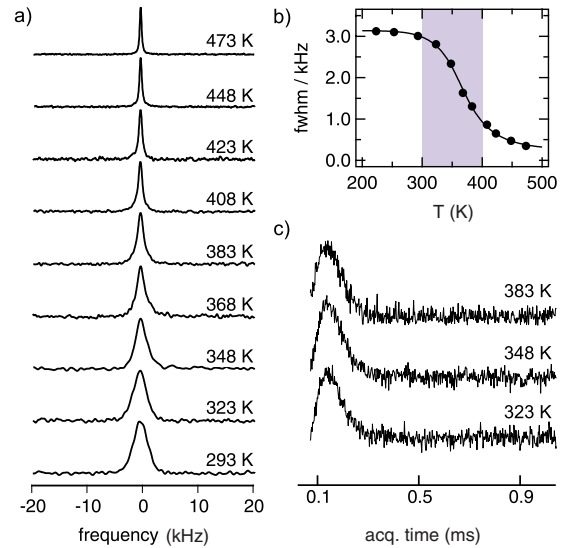

FIG. 1. (Color online) (a) ^{6}Li solid echo NMR spectra of LiAlSi$_2$O$_6$ recorded at various temperatures. (b) Temperature dependence of the line width (full width at half maximum) of the spectra shown in Fig. 1(a). (c) Selected ^{6}Li NMR spin-alignment echoes for temperatures below 400 K. The line widths of the corresponding ^{6}Li SAE NMR spectra are shown in Fig. 1(b) for comparison.

LiAlSi$_2$O$_6$ glass were polished and electrodes of conductive carbon cement were applied. Alternatively, the use of Au electrodes is also possible and gave the same results.[53] The dc conductivity values (σ_{dc}) were determined from the low-frequency plateau of the corresponding impedance spectra which are not shown here for brevity. They agree perfectly with those measured on the same sample earlier, see Fig. 4 in Ref. [50].

III. RESULTS AND DISCUSSION

In Fig. 1(a) ^{6}Li solid echo NMR spectra are shown which were recorded for various temperatures between 293 and 473 K. Starting from the lowest temperature, the NMR line is Gaussian shaped and evolves into a Lorentzian at elevated T due to increasing Li diffusivity. The decrease of the NMR line width (full width at half maximum, FWHM) with increasing temperature, i.e., the so-called motional narrowing (MN), is shown in Fig. 1(b). Significant MN starts at about 325 K. The inflexion point of the curve in Fig. 1(b) is located at $T_{infl.} \approx 375$ K. At this temperature the Li jump rate is approximately given by $\tau_{MN}^{-1} = 2\pi \times \nu_{rl}$ where ν_{rl} is the rigid-lattice line width at $T \rightarrow 0$ K. Inserting $\nu_{rl} \approx 3.1$ kHz yields a hopping rate of about 1.95×10^4 s^{-1} at 375 K. Thus, below this temperature Li correlation rates are equal or smaller than about 10^4 s^{-1} so that they fall in the time window which is accessible by stimulated echo NMR being sensitive to extremely small jump rates.[21–23] Examples of ^{6}Li spin-alignment echoes are displayed in Fig. 1(c). They were recorded at $t_p = 100$ μs and $t_m = 10$ μs. At such a small mixing time the echoes are not influenced by slow Li hopping yet. In Fig. 2 the corresponding ^{6}Li NMR (sin-sin) two-time corre-
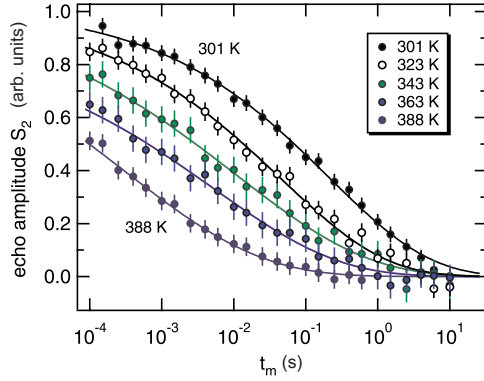
FIG. 2. (Color online) Temperature dependent decay of ^{6}Li spin-alignment echo amplitudes $S_2(t_p,t_m,t)$ of glassy LiAlSi$_2$O$_6$ as a function of mixing time t_m recorded at a radio frequency of 58 MHz. The lines represent fits according to a stretched exponential [see Eq. (1)]. The correlation functions were recorded at a relatively short preparation time of $t_p=100$ μs.

lation functions of LiAlSi$_2$O$_6$ are shown. The echo amplitude S_2, which was read out at $t=t_p=100$ μs, is plotted in a semi-logarithmic presentation as a function of mixing time t_m, which was varied between 100 μs and 10 s. In the case of ^{6}Li with $I=1$, the amplitude of the spin-alignment echo is described by the following two-time phase correlation function[17]

$$S_2(t_p,t_m) = \frac{3}{4}\langle\sin[\omega_Q(t_m=0)t_p]\sin[\omega_Q(t_m)t_p]\rangle. \quad (1)$$

$\langle\ldots\rangle$ denotes the powder average and ω_Q represents the quadrupolar precession frequency. For a spin-1 nucleus it is given by

$$\omega_Q = \frac{3}{4}\pi\delta_Q[3\cos^2\Theta - 1 - \eta\sin^2\Theta\cos(2\Phi)], \quad (2)$$

with the quadrupole coupling constant $\delta_Q=e^2qQ/h$, where h is Planck's constant. e and eq are the proton charge and the principle component of the electric-field gradient tensor, respectively. If electrically inequivalent sites are visited by the jumping ion, the information about the dynamic process is coded in terms of a change in ω_Q. Provided the loss in correlation because of spin-diffusion processes is negligible, as it is practically the case here, the decay of the amplitudes for fixed t_p and variable t_m is in general due to two processes *viz.*, individual jumps of the ions and spin-lattice relaxation. Since the latter process proceeds on a time scale which is more than two orders of magnitude longer than the first one (see below), in the present case the echo amplitude S_2 is exclusively damped by slow Li motions. The data of Fig. 2 were recorded for several temperatures T. Expectedly, with increasing T the inflexion point of the curves shifts to shorter mixing times due to increasing Li diffusivity. The correlation functions do not show single-exponential behavior, instead they can only be parameterized with stretched exponentials according to
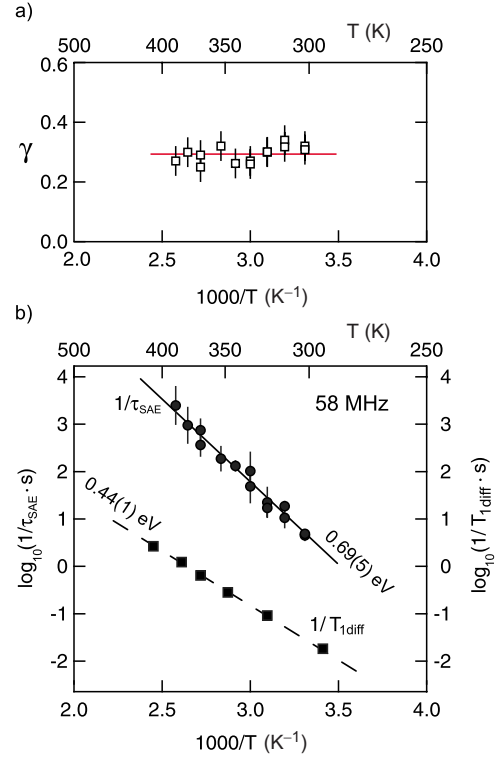

FIG. 3. (Color online) (a) Stretching factor γ of the correlation functions of Fig. 2 as a function of $1/T$. The mean value ($\bar\gamma \approx 0.29$) is represented by the solid line. (b) Temperature dependence of the ^{6}Li spin-alignment echo decay rates τ_{SAE}^{-1} as directly obtained from the two-time correlation functions shown in Fig. 2. Additionally, diffusion induced ^{6}Li NMR spin-lattice relaxation rates are included. Both rates follow Arrhenius behavior but with different slopes.

$$S_2(t_p,t_m,t) = S_{0,t_m\to+\infty} + S_{2,t_m\to0}\exp\left[-\left(\frac{t_m}{\tau_{SAE}}\right)^\gamma\right]. \quad (3)$$

Here, the echo amplitudes are scaled such that they range between 0 and 1 for $t_m\to+\infty$ and $t_m\to0$, respectively. In the temperature range covered by the ^{6}Li SAE NMR measurements, the stretching factor γ turns out to be nearly temperature independent as shown in Fig. 3(a). The mean value $\bar\gamma$ is 0.29(1) between 300 and 390 K. The small stretching factor indicates the presence of a distribution of jump rates and, thus, reflects the complex Li diffusion process in glassy LiAlSi$_2$O$_6$. Correlation functions with nearly the same stretching factor were also observed for LiPO$_3$ glass by Faske *et al.*,[47] quite recently, and ascribed to dynamical heterogeneities rather than to intrinsically nonexponential correlation functions due to, e.g., forward-backward jump processes being certainly of relevance for the fast ions. The logarithm of the corresponding decay rates τ_{SAE}^{-1} of the correlation functions measured at $t_p=100$ μs are plotted vs $1/T$ in Fig. 3(b). $\tau_{SAE}^{-1}(T)$ follows Arrhenius behavior according to

$$\tau_{SAE}^{-1} = \tau_{0,SAE}^{-1}\exp[-E_{a,SAE}/(k_BT)], \quad (4)$$

where k_B is the Boltzmann constant. The activation energy $E_{a,SAE}$ of Li hopping is 0.69(5) eV. The pre-exponential fac-

TABLE I. Comparison of activation energies $E_{a,\text{SAE}}$ and pre-exponential factors τ_0^{-1} for glassy $LiAlSi_2O_6$ obtained from various methods being sensitive either to long- or short-range Li motions

Method	$E_{a,\text{SAE}}$ (eV)	τ_0^{-1} (s^{-1})
^{6}Li SAE NMR[a]	0.69(5)	$1.8(2) \cdot 10^{12}$
^{6}Li SAE NMR[b]	0.76(7)	$3.0(3) \cdot 10^{14}$
^{7}Li SAE NMR[c]	0.58(3)	
^{7}Li SLR NMR[d]	0.44(1)	
^{7}Li SLR NMR[e]	0.77(3)	$4.8(3) \cdot 10^{13}$
Impedance spectroscopy[f]	0.66(2)	
dc conductivity[g]	0.71(2)	$5.6(3) \cdot 10^{13}$

[a]$300 < T < 390$ K; $t_p = 100$ μs.
[b]$290 < T < 400$ K; $t_p = 300$ μs.
[c]$190 < T < 240$ K; $t_p = 10$ μs, Ref. 31.
[d]$295 < T < 420$ K, low-T flank of the SLR peak.
[e]$675 < T < 780$ K, maxima of the SLR peaks recorded at various $\omega_0/2\pi$.
[f]$380 < T < 570$ K, high-T flank of $\rho^{-1}(1/T)$ peaks, Ref. 50.
[g]$345 < T < 560$ K, conversion of σ_{dc} into τ_σ.

tor $\tau_{0,\text{SAE}}^{-1}$ is given by $1.8(2) \times 10^{12}$ s^{-1}. It shows a value which is reasonable for phonon frequencies typically ranging between 10^{12} and 10^{14} s^{-1}. Analogous ^{7}Li SAE NMR measurements, which were performed recently,[31] yielded a somewhat smaller value [0.58(3) eV]. Interestingly, an activation energy $E_{a,\text{SAE}}$ of 0.69 eV agrees with that which was deduced by Roth and Böhm[53] as well as with that obtained by our group from impedance spectroscopy measurements[49,50] on the same sample [0.66(2) eV, 400 K $\leq T \leq$ 575 K, see Fig. 6 in Ref. 50]. In Ref. 50 the logarithm of the resistivity ρ against $1/T$ was plotted to analyze the data. That way, an activation energy was obtained from the high-temperature slope of the resultant $\log_{10}\rho(1/T)$ peak. ρ is proportional to M''/ν where M'' is the imaginary part of the electrical modulus and ν is the corresponding frequency of the impedance measurements. By analyzing just the dc conductivity ($\sigma_{\text{dc}} \cdot T$ vs $1/T$) read out from the corresponding impedance spectra, which we have recorded here between 300 and 800 K for the same sample once again to check the reproducibility of the data, a very similar activation energy of 0.71(2) eV (see below) is obtained, as expected. It should be noted that at similar temperatures the mixing times t_m between 0.1 ms and 10 s correspond to a frequency range for which the conductivity spectra $\sigma(\nu)$ are governed mainly by the dc plateau. Hence, the same time scales are used to measure ion dynamics by the two methods. Furthermore, forward-backward jumps, which are responsible for the dispersive part of the conductivity spectra showing up at higher frequencies, presumably do not contribute to the echo damping, here.

Whereas σ_{dc} measurements are sensitive to ionic motions on a macroscopic length scale, by means of ^{6}Li SAE NMR, long-range diffusion parameters are determined from an atomistic, i.e., microscopic point of view.[24,26] Li motions on a shorter length scale can be probed by (laboratory frame) spin-lattice relaxation NMR.[11,18,19] In Fig. 3(b) the temperature dependence of the Li diffusion induced ^{6}Li NMR spin-lattice relaxation (SLR) rates $1/T_{1\text{diff}}$ of glassy $LiAlSi_2O_6$ are

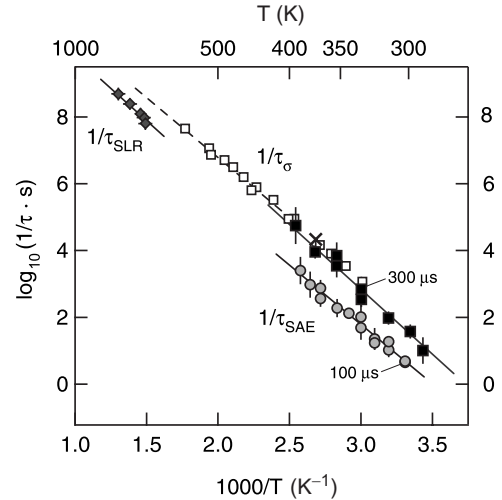FIG. 4. Jump rates as probed by ^{6}Li spin-alignment echo NMR at two different preparation times t_p ($\bullet$: 100 μs, $\blacksquare$: 300 μs) plotted against inverse temperature. For comparison, the rates deduced from the maxima of the diffusion induced ^{7}Li SLR NMR rate peaks ($\blacklozenge$) (see Refs. 48 and 49) as well as those obtained by σ_{dc} measurements ($\blacksquare$) are shown, too. Solid lines show fits according to an Arrhenius relation. The corresponding diffusion parameters are listed in Table I. The estimated jump rate by means of ^{6}Li NMR MN data (see Fig. 1) is shown ($\times$), too.

also shown. The corresponding magnetization transients follow single-exponential time behavior. The ^{6}Li SLR NMR rates were probed at $\omega_0/2\pi = 58$ MHz. As expected, the temperature dependence of $1/T_{1\text{diff}}$ measured at this frequency and in this temperature range, which corresponds to the low-T flank of the diffusion induced rate peak,[18] yields a substantially smaller value $E_{a,\text{SLR}}$, viz., 0.44(1) eV, than probed by SAE NMR. Therefore, it is better to compare $E_{a,\text{SLR}}$ with results from techniques being sensitive to Li motions on a shorter length scale, e.g., with ac conductivity data.[49,50] Moreover, especially the low-T flank of the diffusion induced rate maximum is affected by correlation effects such as structural disorder and/or Coulomb interactions.[54–57] One should note that temperature dependent SLR NMR measurements on different isotopes should not necessarily result in the same activation energy. The characteristics of Li diffusion might be differentially transferred into the primary observable $1/T_{1\text{diff}}$ via the specific properties of the spins under investigation. However, in the present case good agreement is found between activation energies obtained from ^{6}Li [$\approx$0.44 eV at 58 MHz (this work), $\approx$0.43 eV at 28 MHz (this work, but not shown here) and ^{7}Li SLR NMR rates ($\approx$0.39 eV at 38.9 MHz, see Ref. 48).

So far, we have not extended our ^{6}Li NMR measurements up to higher temperatures in order to probe the diffusion induced SLR NMR rate maximum from which the Li jump rate can be determined. However, ^{7}Li SLR NMR data are available on the same sample.[48,49] In Fig. 4 the SAE NMR decay rates recorded at $t_p = 100$ μs and presented in Fig. 3 are shown together with the Li jump rates τ_{SLR}^{-1} which were determined via ^{7}Li SLR NMR measurements.[31,48,49,58] The latter were obtained by recording diffusion induced SLR rates over a broad temperature range and for different radio

frequencies $\omega_0/2\pi$ ranging from 10 to 77 MHz.[31,58] Plotting $\log(1/T_{1\text{diff}})$ vs $(1/T)$ revealed a diffusion induced rate peak for each frequency $\omega_0/2\pi$. The maximum condition $\omega_0\tau_{\text{SLR}} \approx 0.62$ (according to BPP theory[59]) allowed the estimation of τ_{SLR}^{-1} at the temperature T_M where the rate maximum appears. As can be seen from Fig. 4 the resultant rates are in fair agreement with those directly read out from ^{6}Li SAE NMR correlation functions recorded at $t_p = 100$ μs. Although the temperature range covered by the τ_{SLR}^{-1} rates is quite narrow, we fitted an Arrhenius law to the data yielding $E_{a,\text{SLR}} = 0.77(3)$ eV and $\tau_{0,\text{SLR}}^{-1} = 4.8(3) \times 10^{13}$ s^{-1}, respectively. If no deviation from simple Arrhenius behavior is assumed over the whole temperature range, extrapolation of τ_{SLR}^{-1} to lower T reveals that the rates $\tau_{\text{SAE}}^{-1}(t_p = 100$ μs$)$ are somewhat smaller than expected from SLR NMR. As an example, at 390 K the extrapolated rate τ_{SLR}^{-1} is about a factor of 3 larger than τ_{SAE}^{-1} at the same T. In this context it should be noted that the validity of the relation $\omega_0\tau_{\text{SLR}} \approx 0.62$ depends on the type of the underlying correlation function. For instance, if a distribution of correlation times is assumed, e.g., of the Cole-Davidson (CD) type, for which the spectral density function

$$J_{\text{CD}} \propto \omega_0^{-1}(1 + \omega_0^2\tau_{\text{SLR}}^2)^{-\beta_{\text{CD}}/2} \sin[\beta_{\text{CD}} \arctan(\omega_0\tau_{\text{SLR}})] \tag{5}$$

is determined by the width exponent β_{CD}, the BPP maximum condition, mentioned above, is no longer exactly valid. Instead, the product $\omega_0\tau_{\text{SLR}}$ is by a factor of 2 larger if, e.g., $\beta_{\text{CD}} \approx 0.3$ is used. Thus, the corresponding τ_{SLR}^{-1} rate decreases accordingly.[31]

A larger difference is found when both, τ_{SLR}^{-1} and $\tau_{\text{SAE}}^{-1}(t_p = 100$ μs$)$ rates are compared with those values which were obtained from dc conductivity data (see Fig. 4). σ_{dc} is related via the Nernst-Einstein equation[60] to the diffusion coefficient D_{NE} which is related to the tracer diffusion coefficient D_{tr} via the Haven ratio H_R

$$D_{\text{tr}} = H_R \cdot D_{\text{NE}} = H_R \cdot \frac{\sigma_{\text{dc}} \cdot k_B T}{N \cdot q^2}. \tag{6}$$

q is the charge of the Li ions. In order to calculate the number density of charge carriers N in glassy LiAlSi$_2$O$_6$, we have assumed that the density is similar to that of crystalline LiAlSi$_2$O$_6$ (3.2 g cm^{-3}). In fact, it differs by only about a few percent from that in the crystalline state.[48] The macroscopic diffusion coefficient D_{tr} is related via the correlation factor f to the microscopic self-diffusion coefficient, $D_{\text{tr}} = fD_{\text{sd}}$.[60] f reflects the degree of correlated motion of the charge carriers. It ranges between 0 and 1. $f = 1$ is obtained for uncorrelated motion. Further on, D_{sd} can be expressed by the Einstein-Smoluchowski equation for three-dimensional (3D) diffusion, $D_{\text{sd}} = a^2/(6\tau)$.[60] In the following, the rate τ^{-1} in this equation is denoted as τ_σ^{-1} as it is finally obtained from σ_{dc}. The calculated rates for uncorrelated motion are shown in Fig. 4. They were obtained by simply assuming $H_R = 1$ and a mean jump distance a of 0.25 nm as a realistic approximation. In a first approach, jump distances are commonly of this order for a range of materials. The so obtained rates follow an Arrhenius law which is determined by $E_{a,\sigma} = 0.71(2)$ eV

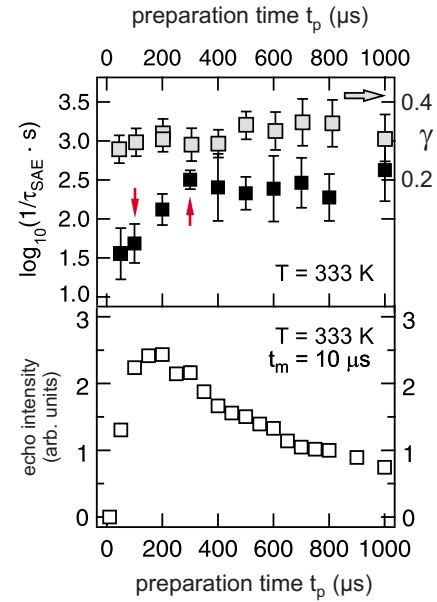FIG. 5. (Color online) *Top*: Dependence of the ^{6}Li SAE NMR decay rate τ_{SAE}^{-1} (filled symbols) on preparation time t_p (left ordinate). The corresponding stretching exponents γ (light gray symbols) are also shown (right ordinate). Data were recorded at $T = 333$ K. *Bottom*: Echo intensity S_2 as a function of preparation time and for fixed mixing time $t_m = 10$ μs. The arrows mark the preparation times with which most of the stimulated-echo experiments were performed.

and $1/\tau_{0,\sigma} = 5.6(3) \times 10^{13}$ s^{-1}. The difference between τ_σ^{-1} and τ_{SLR}^{-1}, obtained when $\tau_\sigma^{-1}(T)$ is extrapolated to higher T according to this Arrhenius relation (dashed line in Fig. 5), is about one order of magnitude. It might be explained by the facts that the two methods probe (i) Li diffusion on different length scales and (ii) via different correlation functions.[54,57,61] Especially in ionic conductors with disordered structure this difference is not so much surprising and had been the topic of numerous experimental and theoretical papers during the last decades, see, e.g., Refs. 49, 57, and 61–68. Consistent rates τ_σ^{-1} and τ_{SLR}^{-1} would be obtained in the present case by, e.g., assuming an unlikely small Haven ratio or even a larger jump distance a.

The difference between the rates τ_{SAE}^{-1} on the one hand and τ_σ^{-1} on the other hand (see Fig. 4) is presumably due to the circumstance that by stimulated echo NMR measurements performed at $t_p = 100$ μs, not all of the Li jumps in the glass are detected. Unsurprisingly, ^{7}Li solid echo NMR spectra[31] of glassy LiAlSi$_2$O$_6$ clearly reveal a broad distribution of electric-field gradients being typical of a disordered material. Since the electric-quadrupole moment of ^{6}Li is by about a factor of 50 smaller than that of ^{7}Li,[46] much larger preparation times are needed in ^{6}Li SAE NMR to resolve jumps between electrically similar Li sites. Therefore, we have recorded ^{6}Li NMR phase correlation functions at preparation times larger than 100 μs in order to enhance the sensitivity of the measurements. This should allow us to detect hopping processes between adjacent Li sites whose quadrupolar precession frequencies differ only slightly due to the charge disorder of the glass. In Fig. 5 the preparation time depen-

dence of the decay rate τ_{SAE}^{-1} is shown. The corresponding two-time correlation functions were recorded for different t_p at $T=333$ K. Starting from $t_p=50$ μs the rate increases by about one order of magnitude until $t_p \approx 300$ μs is reached. For $t_p > 300$ μs no significant dependence of the decay rate on the preparation time is found. This can be interpreted as the signature of a random hopping process in the glass[69] similar to the observations of Vogel *et al.*[40] by ^{109}Ag NMR on a silver phosphate glass. Spin-diffusion effects as well as the presence of small-step diffusion processes in frequency space should result in a characteristic dependence of the decay rate on t_p.[31,69] A decrease of the correlation rate might be explained by motional phase averaging which occurs when t_p reaches the order of the motional correlation time. Therefore, phase averaging is expected to be much more pronounced at even higher preparation times ($t_p > 1$ ms) or temperatures. Such an effect was also found by previous ^{7}Li SAE NMR experiments, see Fig. 14 in Ref. 31, as well as by similar measurements on a glassy Ag$^+$ conductor studied by Böhmer *et al.*[70] The observed t_p independence of the decay rate does not indicate the influence of (strictly) localized motions on the echo decay. Presumably, the changes of the quadrupole frequencies associated with such jump processes are too small in order to be resolved even though the preparation time is chosen to be relatively long, see also Ref. 31. Thus, a nearly constant loss (NCL) phenomenon observed for glassy and crystalline spodumene via ac conductivity measurements[71] performed at temperatures below 273 K seems to be not reflected in the S_2-decay curves. Roughly speaking, Li SAE NMR is a method which is primarily sensitive to successful displacements of the charge carriers rather than to strongly localized (caged) motions (see above).

In Fig. 5 the echo intensity as a function of t_p and for short t_m, i.e., when no significant echo decay has occurred due to Li jumps during t_p, is also shown. The maximum is located around 175 μs. This is in fair agreement with a very recent theoretical study of Böhmer *et al.* predicting the position of the amplitude maximum as a function of t_p and the width of a Gaussian type distribution of frequencies.[72] In this context it should be noted that also the appearance of the echo should not necessarily be expected at $t=t_p$. As quite recently pointed out, significant time shifts from the position $t=t_p$ can be observed if the dephasing times are much smaller than the inverse rigid-lattice line width Σ of the spectrum [see Fig. 1(a)]. The latter is about 330 μs in the present case. This can already be seen in Fig. 1(c) and is in detail shown in Fig. 6 where we have plotted the position of the observed ^{6}Li stimulated echo as a function of preparation time t_p set. At short t_p the shift is approximately 160 μs. This is in good agreement with the theoretical prediction of $1/\varsigma$ with $\varsigma \approx 2.668 \times \Sigma$. ς^2 denotes the variance of the underlying Gaussian distribution of quadrupole frequencies.

Going back to the result of Fig. 5, it can be seen that for $t_p \geq 100$ μs SAE NMR measurements are reasonable. The difference between τ_{SAE}^{-1} recorded at $t_p=100$ μs and $t_p=300$ μs, respectively, is shown in Fig. 4 for the whole temperature range studied here. The shape of the corresponding correlation functions is very similar to that shown in Fig. 2 for $t_p=100$ μs. The mean stretching factor slightly decreases to 0.28. The two preparation times chosen refer to the range
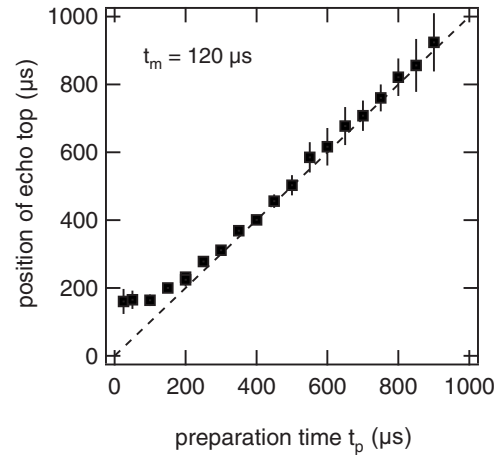

FIG. 6. Position of the ^{6}Li stimulated-echo top as a function of preparation time. The deviation from the expected echo position at $t=t_p$ for sin-sin time-domain signals is explicitly treated in Ref. 72. Data were recorded at a constant mixing time t_m of 120 μs. The smaller the echo intensity, the larger the error in determining the echo position.

for which the echo amplitude is maximal. Whereas the τ_σ^{-1} values are consistent with the SAE NMR rates recorded at larger t_p, the rates τ_{SLR}^{-1} of Fig. 4—obtained after extrapolation to lower temperatures—take an intermediate position between $\tau_{SAE}^{-1}(t_p=100$ μs) and $\tau_{SAE}^{-1}(t_p=300$ μs), respectively. Let us note that the jump rates $\tau_M^{-1}(T)$ obtained from the analysis of the electrical modulus $M''(\nu)$ spectra (not shown for brevity, here) are in reasonable agreement with the values τ_σ^{-1} and thus τ_{SAE}^{-1}. τ_M^{-1} rates were determined from the maxima of various M'' peaks between 290 and 500 K taking into account a stretched exponential as underlying correlation function.[73] Interestingly, analyzing the data according to $M'' \propto \omega\tau_M/[1+(\omega\tau_M)^{(2-n_\sigma)}]$ with $\omega/2\pi=\nu$ leads to a stretching factor $1-n_\sigma=0.27(1)$ which is in good agreement with γ obtained from SAE NMR.[74] The relation $\gamma E_{a,\sigma}/E_a \propto 1$ introduced by Ngai *et al.*[75,76] is fulfilled when E_a is identified with the low-T activation energy (0.17–0.23 eV) of the $\log_{10}\rho(1/T)$-peaks as presented in Ref. 50 for frequencies between 10 kHz and 10 MHz.

Up to here, we focused on the decay rates τ_{SAE}^{-1} which can be directly obtained from the S_2 decay, but without further considering the stretching exponent γ being related to the width of the distribution of jump rates. In a first approach the Γ-function[77] can be used to transform the rates τ_{SAE} into the mean values $\langle\tau_{SAE}\rangle$ according to $\langle\tau_{SAE}\rangle(T) = [\tau_{SAE}(T)/\gamma(T)]\{\Gamma[1/\gamma(T)]\}$ (see Fig. 7). Since γ is almost temperature independent for both the measurements at $t_p=100$ μs and $t_p=300$ μs, the corresponding activation energies remain unchanged. However, in both cases the rates are shifted to lower values by about one order of magnitude (Fig. 7), i.e., $\langle 1/\tau_{SAE}\rangle(t_p=300$ μs) does no longer fit to the τ_σ^{-1} rates shown in Fig. 4. In Ref. 31 ^{7}Li SAE NMR decay rates are presented which were measured at a short preparation time of 10 μs and transformed afterwards via the same procedure into the mean values. Interestingly, for the ^{7}Li two-time (sin-sin) correlation functions the same stretching factor was found $[\bar{\gamma}(^7\text{Li})=0.3(1)]$ as for the corresponding ^{6}Li
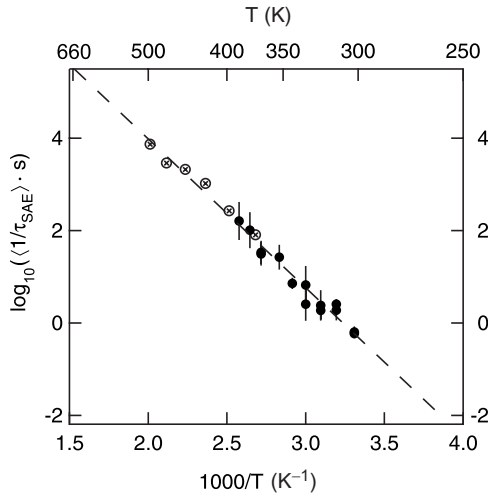
FIG. 7. Mean SAE NMR decay rates of $LiAlSi_2O_6$ obtained via ^6Li (●) and ^7Li (⊗) NMR two-time correlation functions measured at $t_p = 100$ μs and $t_p = 10$ μs, respectively. The latter were taken from Ref. 31. The dashed line represents an Arrhenius fit and yields an overall activation energy of about 0.64 eV.

S_2-decay curves measured here $[\bar{\gamma}(^6Li) = 0.29(1)]$. In order to be able to compare the ^7Li SAE NMR results with our ^6Li data we converted the rates measured at $t_p = 100$ μs into mean values, too. The result is shown in Fig. 7. Good agreement is obtained with the recently published data. Considering all the rates shown in Fig. 7, an overall activation energy of 0.64(2) eV is obtained which agrees with that from dc conductivity measurements.

Finally, we started to record ^6Li SAE NMR two-time correlation functions of a sample which was prepared by heating pieces of the glass at about 750 K for a few days. The slabs of the so produced crystalline sample, which shows the β-spodumene structure, were used previously for ^7Li SLR NMR and impedance spectroscopy measurements, see Refs. 48 and 50 for details. In contrast to the SAE NMR measurements on the glassy sample, the two-time correlation functions of the crystalline sample obtained by the heating program are much less stretched. The corresponding temperature independent stretching factor was about 0.78(5). The γ parameter determining the shape of the correlation functions may be interpreted as a measure of the variance of the underlying distribution of jump rates. A value of ≈ 0.8 clearly indicates a much smaller distribution of jump rates in the crystalline material with its structurally disordered Al^{3+}/Si^{4+} sublattice. In turn, the larger stretching exponent already reveals the much more complex Li diffusion behavior of the glassy material ($\gamma \approx 0.3$). The smaller the width parameter γ, the broader the corresponding distribution.[78] Provided that the observed strong deviation from exponential time behavior is solely due to heterogeneous dynamics in the glass, $\gamma \approx 0.3$ indicates a distribution half width of several orders of magnitude, see, e.g., Refs. 78 and 47.

In Fig. 8 the decay rates τ_{SAE}^{-1} of crystalline $LiAlSi_2O_6$ are shown together with τ_{SLR}^{-1} estimated from the diffusion induced ^7Li SLR NMR rate maxima recorded at different radio frequencies[31,48,58] as well as τ_σ^{-1} obtained from impedance spectroscopy measurements. For the latter the dc conductiv-
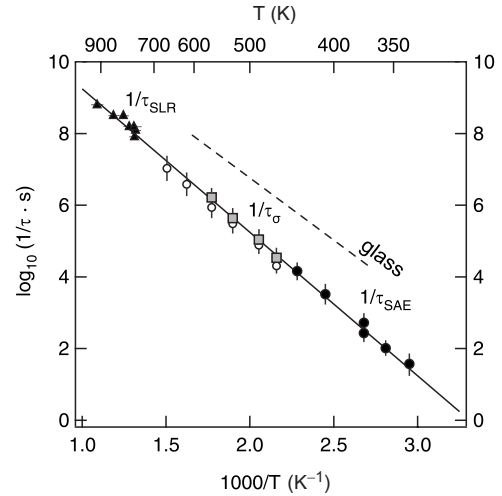

FIG. 8. Li jump rates of $LiAlSi_2O_6$ after heat treatment of the glassy specimens at 750 K for a few days. ^6Li SAE NMR jump rates were measured at $t_p = 300$ μs and 58 MHz. The rates τ_{SLR}^{-1} of this sample are taken from Ref. 58. For comparison, τ_σ^{-1} values are also included, which were deduced from σ_{dc} (nonfilled circles) as well as from analyzing the impedance data in a complex plane diagram (gray filled squares); see text for further details. The solid line represents an Arrhenius fit and yields 0.80(1) eV. It takes only the NMR data into account. The dashed line roughly indicates the Li jump rates ($1/\tau_\sigma$) of glassy $LiAlSi_2O_6$ (see Fig. 5).

ity values were transformed via the Nernst-Einstein and Einstein-Smoluchowski equations into Li jump rates. As for the glass, we used $f = H_R = 1$ and $a = 0.25$ nm (see above). Additionally, we have analyzed the measured impedance data in the complex plane representation by means of equivalent circuit software. In this way it is possible to separate the conductivity of the bulk from the total one which includes also contributions from grain boundaries acting as blocking barriers for long-range Li hopping. Subsequent transformation of the bulk conductivities into jump rates shows that these are just slightly larger than those deduced from σ_{dc}. This indicates the absence of a large volume fraction of blocking grain boundaries in the annealed sample which was directly prepared from the glass specimen without prior milling the source material. Since γ of the crystallized sample is relatively high, the difference between $\langle\tau_{SAE}\rangle$ and τ_{SAE} is negligible. Contrary to the glassy sample, the differently probed jump rates of the crystalline one follow the same Arrhenius law determined by an activation energy of 0.80(1) eV and a pre-exponential factor of $1.75(5) \cdot 10^{13}$ s^{-1}. This activation energy is in very good agreement with that found previously for single crystalline β spodumene by Roth and Böhm (0.81 eV). However, in single crystalline β-$LiAlSi_2O_6$ the Li jump rates are shifted to smaller values by a factor of about two. For comparison, in Fig. 8 the position of τ_σ^{-1} of glassy $LiAlSi_2O_6$ is indicated by the dashed line. It clearly reveals that Li diffusivity in the glassy form is higher than that in the corresponding crystalline material of the same chemical composition. This was also found for other Li conductors, see, e.g., Refs. 9, 12, and 79–81, and is in good agreement with our previous studies[48–50] on this system.

IV. SUMMARY AND CONCLUSION

Glassy $LiAlSi_2O_6$ with natural abundance was investigated by solid echo ^6Li and two-time ^6Li SAE NMR spectroscopy. Motional narrowing of the ^6Li NMR line width indicates extremely slow Li jumps in glassy $LiAlSi_2O_6$ with rates smaller than 10^4 s^{-1} below $T = 400$ K. We have recorded ^6Li two-time sin-sin hopping correlation functions at fixed t_p and for variable t_m between 300 and 400 K. The echo damping is solely due to slow Li jumps. The diffusion process in the glass is characterized by strongly nonexponential correlation functions indicating the presence of an expectedly broad distribution of jump rates. In particular, Li jump rates obtained from ^6Li spin-alignment echo NMR measurements carried out at a preparation time of 300 μs agree perfectly with those which can be roughly estimated from dc conductivity measurements probing long-range diffusion parameters. This evidences that both experiments are governed by the same correlation function which is determined by diffusion of single ions. This is in contrast to SLR NMR whose underlying correlation function seems to be quite different from that probed by conductivity and SAE NMR experiments.

As shown quite recently for ^7Li, see Ref. 24, and corroborated for ^6Li on a Li_3N single crystal (Ref. 26) as well as by a subsequent study by Faske *et al.* on $LiPO_3$ glass,[47] the measurement of ^6Li stimulated echoes provides access to long-range diffusion parameters probed directly, i.e., without involving a model, by means of a microscopic technique.

Expectedly, the $LiAlSi_2O_6$ sample obtained after devitrification exhibited a much smaller distribution of Li jump rates, as indicated by the less stretched two-time correlation functions. Once again, good agreement between the diffusion parameters obtained by SAE NMR and dc conductivity is found. Interestingly, also the Li jump rates obtained from spin-lattice relaxation NMR carried out at different resonance frequencies agree with these results.

*To whom correspondence should be addressed; wilkening @pci.uni-hannover.de

†heitjans@pci.uni-hannover.de

[1] P. G. Bruce, B. Scrosati, and J.-M. Tarascon, Angew. Chem., Int. Ed. **47**, 2930 (2008).

[2] A. S. Aricò, P. Bruce, B. Scrosati, J.-M. Tarascon, and W. V. Schalkwijc, Nat. Mater. **4**, 366 (2005).

[3] M. S. Whittingham, Chem. Rev. (Washington, D.C.) **104**, 4271 (2004).

[4] *Lithium Batteries Science and Technology*, edited by G.-A. Nazri and G. Pistoia (Kluwer, Dordrecht/Plenum, Boston, 2004).

[5] B. Scrosati, Nature (London) **373**, 557 (1995).

[6] L. Nazar, G. Goward, F. Leroux, M. Duncan, H. Huang, T. Kerr, and J. Gaubicher, Int. J. Inorg. Mater. **3**, 191 (2001).

[7] J. M. Tarascon and M. Armand, Nature (London) **414**, 359 (2001).

[8] *Lithium Ion Batteries—Fundamentals and Performance*, edited by M. Wakihara and O. Yamamoto (Wiley, Weinheim, 1998).

[9] P. Heitjans and S. Indris, J. Phys.: Condens. Matter **15**, R1257 (2003).

[10] A. V. Chadwick and S. L. P. Savin, Solid State Ionics **177**, 3001 (2006).

[11] P. Heitjans, S. Indris, and M. Wilkening, in *Nanocomposites—Ionic Conducting Materials and Structural Spectroscopies*, Electronic Materials: Science & Technology Vol. 10, edited by P. Knauth and J. Schoonman (Springer, New York, 2007), Chap. 7, pp. 227–246.

[12] P. Heitjans, M. Masoud, A. Feldhoff, and M. Wilkening, Faraday Discuss. **134**, 67 (2007).

[13] P. Knauth and H. L. Tuller, Solid State Ionics **85**, 1654 (2002).

[14] M. Wilkening, V. Epp, A. Feldhoff, and P. Heitjans, J. Phys. Chem. C **112**, 9291 (2008).

[15] J. F. Stebbins, Chem. Rev. (Washington, D.C.) **91**, 1353 (1991).

[16] D. Brinkmann, Prog. Nucl. Magn. Reson. Spectrosc. **24**, 527 (1992).

[17] R. Böhmer, K. Jeffrey, and M. Vogel, Prog. Nucl. Magn. Reson. Spectrosc. **50**, 87 (2007).

[18] P. Heitjans, A. Schirmer, and S. Indris, in *Diffusion in Condensed Matter—Methods, Materials, Models*, 2nd ed., edited by P. Heitjans and J. Kärger (Springer, Berlin, 2005), Chap. 9, pp. 369–415.

[19] P. Heitjans, S. Indris, and M. Wilkening, Diffus. Fundam. **45**, 2 (2005).

[20] M. Wilkening and P. Heitjans, Defect Diffus. Forum **237-240**, 1182 (2005).

[21] M. Wilkening, W. Küchler, and P. Heitjans, Phys. Rev. Lett. **97**, 065901 (2006).

[22] M. Wilkening and P. Heitjans, J. Phys.: Condens. Matter **18**, 9849 (2006).

[23] M. Wilkening and P. Heitjans, Solid State Ionics **177**, 3031 (2006).

[24] M. Wilkening, C. Mühle, M. Jansen, and P. Heitjans, J. Phys. Chem. B **111**, 8691 (2007).

[25] M. Wilkening, R. Amade, W. Iwaniak, and P. Heitjans, Phys. Chem. Chem. Phys. **9**, 1239 (2007).

[26] M. Wilkening, D. Gebauer, and P. Heitjans, J. Phys.: Condens. Matter **20**, 022201 (2008).

[27] M. Wilkening and P. Heitjans, Phys. Rev. B **77**, 024311 (2008).

[28] R. Böhmer, T. Jörg, F. Qi, and A. Titze, Chem. Phys. Lett. **316**, 419 (2000).

[29] F. Qi, T. Jörg, and R. Böhmer, Solid State Nucl. Magn. Reson. **22**, 484 (2002).

[30] F. Qi, G. Diezemann, H. Böhm, J. Lambert, and R. Böhmer, J. Magn. Reson. **169**, 225 (2004).

[31] F. Qi, C. Rier, R. Böhmer, W. Franke, and P. Heitjans, Phys. Rev. B **72**, 104301 (2005).

[32] R. Böhmer and F. Qi, Solid State Nucl. Magn. Reson. **31**, 28 (2007).

[33] Z. Xu and J. F. Stebbins, Science **270**, 1332 (1995).

[34] V. W. J. Verhoeven, I. M. de Schepper, G. Nachtegaal, A. P. M. Kentgens, E. M. Kelder, J. Schoonman, and F. M. Mulder, Phys. Rev. Lett. **86**, 4314 (2001).

[35] J. Cabana, N. Dupré, G. Rousse, C. P. Grey, and M. R. Palacin, Solid State Ionics **176**, 2205 (2005).

[36] L. S. Cahill, R. Chapman, J. Britten, and G. Goward, J. Phys. Chem. B **110**, 7171 (2006).

[37] L. S. Cahill, C. W. Kirby, and G. Goward, J. Phys. Chem. B **112**, 2215 (2008).

[38] L. van Wüllen, T. Echelmeyer, H.-W. Meyer, and D. Wilmer, Phys. Chem. Chem. Phys. **9**, 3298 (2007).

[39] R. Böhmer, J. Magn. Reson. **147**, 78 (2000).

[40] M. Vogel, C. Brinkmann, H. Eckert, and A. Heuer, Phys. Chem. Chem. Phys. **4**, 3237 (2002).

[41] M. Vogel, C. Brinkmann, H. Eckert, and A. Heuer, J. Non-Cryst. Solids **307-310**, 971 (2002).

[42] M. Vogel, C. Brinkmann, H. Eckert, and A. Heuer, Phys. Rev. B **69**, 094302 (2004).

[43] D. Schaefer, J. Leisen, and H. Spiess, J. Magn. Reson. **115**, 60 (1995).

[44] K. Schmidt-Rohr and H. Spiess, *Multidimensional Solid-State NMR and Polymers* (Academic, London, 1994).

[45] H. W. Spiess, J. Chem. Phys. **72**, 6755 (1980).

[46] N. J. Stone, At. Data Nucl. Data Tables **90**, 75 (2005).

[47] S. Faske, H. Eckert, and M. Vogel, Phys. Rev. B **77**, 104301 (2008).

[48] W. Franke and P. Heitjans, Ber. Bunsenges. Phys. Chem. **96**, 1674 (1992).

[49] W. Franke, P. Heitjans, B. Munro, and M. Schrader, in *Defects in Insulating Materials*, edited by O. Kanert and J.-M. Spaeth (World Scientific, Singapore, 1993), p. 1009.

[50] B. Munro, M. Schrader, and P. Heitjans, Ber. Bunsenges. Phys. Chem. **96**, 1781 (1992).

[51] E. Fukushima and S. Roeder, *Experimental Pulse NMR* (Addison-Wesley, Reading, MA, 1981).

[52] J. Jeener and P. Broekaert, Phys. Rev. **157**, 232 (1967).

[53] G. Roth and H. Böhm, Ber. Bunsenges. Phys. Chem. **22**, 253 (1987).

[54] K. Funke, Prog. Solid State Chem. **22**, 111 (1993).

[55] K. L. Ngai, Comments Solid State Phys. **9**, 141 (1980).

[56] M. Meyer, P. Maass, and A. Bunde, Phys. Rev. Lett. **71**, 573 (1993).

[57] A. Bunde, W. Dieterich, P. Maass, and M. Meyer, in *Diffusion in Condensed Matter—Methods, Materials, Models*, 2nd ed., edited by P. Heitjans and J. Kärger (Springer, Berlin, 2005), Chap. 20, pp. 813–856.

[58] W. Franke, Ph.D. thesis, University of Hannover, 1993.

[59] N. Bloembergen, E. M. Purcell, and R. V. Pound, Phys. Rev. **73**, 679 (1948).

[60] *Diffusion in Condensed Matter—Methods, Materials, Models*, 2nd ed., edited by P. Heitjans and J. Kärger (Springer, Berlin, 2005).

[61] K. L. Ngai, J. Chem. Phys. **98**, 6424 (1993).

[62] M. Tatsumisago, C. A. Angell, and S. W. Martin, J. Chem. Phys. **97**, 6968 (1992).

[63] O. Kanert, R. Küchler, K. L. Ngai, and H. Jain, Phys. Rev. B **49**, 76 (1994).

[64] K. Ngai and O. Kanert, Solid State Ionics **53-56**, 936 (1992).

[65] K. L. Ngai, Phys. Rev. B **48**, 13481 (1993).

[66] V. Blache, J. Förster, H. Jain, O. Kanert, R. Küchler, and K. Ngai, Solid State Ionics **113-115**, 723 (1998).

[67] M. Meyer, P. Maass, and A. Bunde, J. Non-Cryst. Solids **172-174**, 1292 (1994).

[68] I. Svare, F. Borsa, D. R. Torgeson, and S. W. Martin, J. Non-Cryst. Solids **172-174**, 1300 (1994).

[69] B. Geil, G. Diezemann, and R. Böhmer, J. Chem. Phys. **128**, 114506 (2008).

[70] S. Berndt, K. R. Jeffrey, R. Küchler, and R. Böhmer, Solid State Nucl. Magn. Reson. **27**, 122 (2005).

[71] A. K. Rizos, J. Alifragis, K. L. Ngai, and P. Heitjans, J. Chem. Phys. **114**, 931 (2001).

[72] R. Böhmer, S. Faske, and B. Geil, Solid State Nucl. Magn. Reson. (to be published 2008).

[73] C. T. Moynihan, J. Non-Cryst. Solids **203**, 359 (1996).

[74] It should be noted that according to standard theory the stretching parameter γ is related to the frequency dependence α of the diffusion induced SLR rate in the regime $\omega_0\tau_{\mathrm{SLR}} \gg 1$ by $\alpha = 1 + \gamma$, see, e.g., Refs. 61, 64, and 82. However, for LiAlSi$_2$O$_6$ a sublinear frequency dependence $T_{1\mathrm{diff}}^{-1} \propto \omega_0^{-\alpha}$ with $\alpha = 0.8(1)$ (glass) and $\alpha = 0.9(2)$ (crystal), respectively, was observed (Ref. 48). Thus, the common relation $\alpha = 1 + \gamma$ does not hold in the present case.

[75] K. L. Ngai and S. W. Martin, Phys. Rev. B **40**, 10550 (1989).

[76] K. L. Ngai, G. N. Greaves, and C. T. Moynihan, Phys. Rev. Lett. **80**, 1018 (1998).

[77] E. Artin, *The Gamma Function* (Holt, Rinehart, and Winston, New York, 1964).

[78] C. P. Lindsey and G. D. Patterson, J. Chem. Phys. **73**, 3348 (1980).

[79] M. Wilkening, D. Bork, S. Indris, and P. Heitjans, Phys. Chem. Chem. Phys. **4**, 3246 (2002).

[80] T. Matsuo, M. Shibasaki, N. Saito, and T. Katsumata, J. Appl. Phys. **79**, 1903 (1996).

[81] T. Matsuo, M. Shibasaki, T. Katsumata, and Y. Onoda, Jpn. J. Appl. Phys., Part 1 **33**, 3913 (1994).

[82] P. Freiländer, P. Heitjans, H. Ackermann, B. Bader, C. Kiese, A. Schirmer, H. Stöckmann, and C. V. der Marel, Z. Phys. Chem., Neue Folge **151**, 93 (1987).